Lawrence Berkeley National Laboratory

Lawrence Berkeley National Laboratory

Title

Functional self-assembling bolaamphiphilic polydiacetylenes as colorimetric sensor scaffolds

Permalink

https://escholarship.org/uc/item/6pb4d59j

Authors

Song, Jie
Cisar, Justin S.
Bertozzi, Carolyn R.

Publication Date

2004-05-28

eScholarship.org Powered by the California Digital Library
University of California

Functional self-assembling bolaamphiphilic polydiacetylenes as colorimetric sensor scaffolds

Jie Song[¶,§], *Justin S. Cisar*[‡] *and Carolyn R. Bertozzi*[¶,‡,#,$,§]

Materials Sciences Division, Lawrence Berkeley National Laboratory[¶], Departments of Chemistry[‡] and Molecular and Cell Biology[#], and Howard Hughes Medical Institute[$], University of California, Berkeley, California 94720

Submitted on November 26, 2003; revised on April 9, 2004.

TITLE RUNNING HEAD: Self-assembling bolaamphiphilic polydiacetylenes

[§] Correspondence should be sent to: jsong@lbl.gov (J. Song), bertozzi@cchem.berkeley.edu (C. R. Bertozzi)

ABSTRACT. Conjugated polymers capable of responding to external stimuli by changes in optical, electrical or electrochemical properties can be used for the construction of direct sensing devices. Polydiacetylene-based systems are attractive for sensing applications due to their colorimetric response to changes in the local environment. Here we present the design, preparation and characterization of self-assembling functional bolaamphiphilic polydiacetylenes (BPDAs) inspired by Nature's strategy for membrane stabilization. We show that by placing polar headgroups on both ends of the diacetylene lipids in a transmembranic fashion, and altering the chemical nature of the polar surface residues, the conjugated polymers can be engineered to display a range of radiation-, thermal- and pH-induced colorimetric responses. We observed dramatic nanoscopic morphological

transformations accompanying charge-induced chromatic transitions, suggesting that both side chain disordering and main chain rearrangement play important roles in altering the effective conjugation lengths of the poly(ene-yne). These results establish the foundation for further development of BPDA-based colorimetric sensors.

Introduction:

The past two decades have witnessed significant progress in applying the principles of self-assembly and molecular recognition to the development of biomimetic functional materials.[1] The intrinsic order and unique optical properties of self-assembling polydiacetylenes (PDAs), for instance, have attracted attention to these materials for direct sensing applications.[2,3] When properly aligned, diacetylene groups undergo UV-induced photopolymerization to form an ene-yne alternating polymer chain, resulting in organized structures (Fig. 1). Amphiphilic diacetylene lipids have been polymerized to form single crystals,[4,5] Langmuir-Blodgett films,[3,6-8] self-assembled monolayers,[9] and vesicles[10-13] and ribbons[14,15] in aqueous solution. Recently, immobilization of disulfide-modified PDA vesicles on gold surfaces[16] and amine-terminated vesicles on aldehyde-functionalized glass slides[17] were reported. The conjugated PDA backbone has two major spectroscopically distinct phases designated as the "blue phase" and the "red phase", showing absorption peaks around 630-640 nm and 540-550 nm, respectively. PDA systems can display a combination of these phases that depends on their monomer structures and packing arrangement. Upon external perturbation, such as heat[18,19] or mechanical stress,[20] the conjugated poly(ene-yne) backbone can undergo a drastic reversible or irreversible change in the relative intensity of these two phases. This unique chromatic property has also made polydiacetylenes promising candidates for colorimetric biosensors.[2,3,21]

The architectures of amphiphilic PDA-based colorimetric biosensors reported to date were either vesicles in aqueous solutions[2,13] or thin films on solid supports generated using Langmuir-Blodegtt or Langmuir-Schaefer methods, and incorporated ligands for detection of receptor binding

(Fig. 1).[2,21,22] PDA sensors based on ribbon morphologies have not yet been explored. These sensors integrated molecular recognition and signal transduction into one supramolecular assembly, and responded to binding events by a straightforward color change. The unique device-free detection feature of these colorimetric sensors could allow for on-site detection of biological hazards and offers great potential for a variety of medical or household diagnostic applications.

To fully realize their potential in sensing devices, however, some limitations of present PDA systems must be overcome. First, conventional PDA films or vesicles can respond to a number of external factors, including temperature,[13] solution pH and salt concentration.[12,23] This may be useful for sensing such parameters but can also interfere with biosensing applications as some biological analytes may require a non-physiological pH and/or temperature. Second, the fabrication of thin-film-based sensors requires the Langmuir-Blodgett technique. Finally, there is room for improvement of the sensitivity of the system.

We have previously reported the preliminary characterization of a bolaamphiphilic PDA (BPDA) assembly comprising lipids functionalized with polar headgroups on both ends.[24] An advantage of this system is that the bolaamphiphile self-assembles under mild conditions and can be photo-crosslinked into robust polymer ribbons with a crystalline (hexagonal or pseudo-rectangular) lipid packing arrangement. Here, we report the design, preparation and characterization of BPDAs terminated with different polar functionalities. We varied the chemical nature, including the ability to form hydrogen-bonds, charge and electrostatic interactions, of the headgroups of the bolaamphiphiles and studied their reponses to radiation dose, pH and thermal changes. An understanding of the optical and morphological responses of these BPDAs to environmental perturbations will provide the platform for specific biosensor design.

Results:

As shown in Figure 2, *L*-aspartic acid, *L*-lysine, *L*-serine and ethanolamine were attached to one end of a diacetylene-containing lipid, 10,12-docosadiynedioic acid, through an amide linkage to form

bolaamphiphiles **1**, **2**, **3** and **4**, respectively. These surface residues differ in their charge and hydrogen bonding capabilities. The diacetylene unit was placed at the center of all four bolaamphiphililes to promote the proper alignment of diacetylenes irrespective of their packing arrangement (i.e. parallel or antiparallel).[13,24]

The common intermediate for all four target lipids, N-hydroxysuccinimide-activated bolaamphiphilic lipid **5**, was prepared as previously reported.[24] As shown in Scheme 1, this lipid intermediate was coupled with unprotected *L*-serine and ethanolamine to give **3** and **4**, respectively, in good yields. Diethyl *L*-aspartate hydrochloride[25] was coupled with **5** to give, after deprotection, monomer **1** in moderate overall yield (36%). Higher yields were obtained using a solid-phase approach in which 10,12-docosadiynedioic acid was coupled to Wang resin at one end, followed by coupling with diethyl *L*-aspartate hydrochloride at the other. The coupling of *L*-lysine to **5** was carried out using an ε-NH_2-protected lysine analog, which upon standard deprotection gave compound **2**. The moderate yield (46%) obtained in the last step was due to unintended polymerization during workup and purification.

With compounds **1-4** in hand, we generated polymerized assemblies and analyzed their optical properties. The compounds were suspended in aqueous NaCl solution and sonicated, then incubated at 4 °C for 40 min and polymerized with UV light (254 nm) at varying radiation doses. The resulting polymer solutions were analyzed by absorption spectroscopy. As shown in Figure 3A, after a 0.1 J/cm^2 radiation, **BPDA-3**, terminated with *L*-serine surface residues, absorbs mainly at 630 nm and gives a blue color (Fig. 3B). The other three BPDAs, terminated with ethanolamine, *L*-lysine and *L*-aspartate residues on one end of the bolaamphiphilic lipids, absorb more intensely at 540-550 nm (the "red phase"), displaying various shades of blue (for **BPDA-2** and **BPDA-4**) and purple (for **BPDA-1**) (Fig. 3B).

The different spectral intensities shown in Figure 3A suggest that the extent of polymerization of BPDAs vary. By applying UV irradiation for a longer time, we did observe an increase in optical density for all BPDAs, most notably when the radiation dose increased from 0.05 to 0.2 J/cm^2 (data

not shown). It is known, however, that extended irradiation can increase the amount of "red phase" polydiacetylene.[13] Indeed, as shown in Figure 3C, we observed a radiation dose-dependent blue-to-red optical shift for all of BPDAs tested. For all subsequent experiments, BPDAs were prepared with a 0.1 J/cm^2 radiation dose which was deemed optimal for maximizing the combination of polymerization and "blue-phase" composition.

One practical consideration in the design of colorimetric biosensors is to minimize the colorimetric response (CR) to environmental perturbations other than the ligand-receptor binding events. Two leading contributors to false positive responses are pH- and temperature-induced CR. To determine the CR of BPDAs to pH and thermal perturbations, we subjected all four BPDA systems to acid and base treatments as well as temperature elevations. These BPDA systems showed very different pH- and temperature-induced CRs, sometimes accompanied by dramatic morphological transformations on a nanoscopic level. As shown in Figure 4, **BPDA-1** demonstrated the most sensitive blue-to-red CR in response to base exposure, with a 20% CR at physiological pH (pH 7.4). At pH 8.5, the CR of **BPDA-1** dramatically increased to 50%, and then leveled off at 80% at pH 11. In contrast, the other three BPDAs showed negligible background CR between pH 6 and pH 7.4 (Fig. 4). To induce a 50% CR, pH 10.5 and 10 were required for **BPDA-2** and **BPDA-3**, respectively. The CR of **BPDA-4** never reached 50% even at pH 14. The pH-induced CR of **BPDA-1** was also accompanied by a dramatic morphological transformation from polymer ribbons to nanofibers, as shown in Figure 5 (row A, columns 1 and 2). Similarly, the base-induced CR observed with **BPDA-2** and **BPDA-3** was also accompanied by a ribbon-to-nanofiber morphological transition (Fig. 5, rows B and C, columns 1 and 2). Base-induced CR of **BPDA-4,** which bears a neutral surface moiety, was accompanied by a less dramatic morphological change from wide ribbons to narrower ones, within the time frame of the TEM sample preparation (~ 1 min) (Fig. 5, row D, columns 1 and 2). No significant optical (Fig. 4) or morphological (Fig. 5, column 3) response was observed when acids were added to freshly formed BPDAs, with the exception of **BPDA-2** where a less than 10% CR along with mild splitting of wider ribbons into narrower ones were observed upon the acid treatment.[24]

The thermally-induced CRs of BPDAs are shown in Figure 6. Similar to the trend observed for pH-CR curves, **BPDA-1** showed the most sensitive response to temperature increases (~ 80% at 60 ºC). The other three BPDA systems were relatively resistant to thermal perturbations, with less than 10% CR at 50 ºC. Among all, **BPDA-3** demonstrated the greatest thermal stability, maintaining less than 20% CR even at 80 ºC. It is interesting to note, however, that none of the thermally-induced optical responses of BPDAs were accompanied by ribbon-to-nanofiber morphological transformation. The ribbon-like morphologies of all BPDAs were preserved upon heat activation (data not shown).

Discussion:

A fundamental goal in the design of biosensors is to establish an effective transduction pathway from binding of a biological analyte to signal output. For self-assembling PDA-based biosensors, this requires a balance between the rigidity and flexibility of the sensor scaffold. A lipid sensor scaffold with crystalline packing that can be perturbed to the more fluid state upon analyte binding should maximize the optical output of PDA-based biosensors.

In nature, membrane-spanning lipids endow archaebacteria, a class of microorganisms that can resist extreme environmental conditions such as low pH, high temperature, and high salt, with extraordinary membrane stability.[26] Mimicking Nature, we previously showed that the use of bolaamphiphilic instead of amphiphilic diacetylene lipids could rigidify the packing arrangement of the self-assembling polymer scaffold.[24] In addition, it was demonstrated that various degrees of fluidity may be introduced into the rigid BPDA system via proper lipid doping,[22] making BPDAs attractive candidates for building colorimetric biosensors. However, a general strategy to control the background colorimetric response of BPDA-based biosensors to environmental perturbations, including pH and temperature, was lacking. Here, we exploit various intermolecular interactions including electrostatic, hydrogen bonding, and van der Waals, in the design of functional BPDAs for biosensing applications, in an effort to elucidate design parameters that determine the initial color and the pH and thermal

responsiveness of these polymers.

We have shown that the chemical nature of the functional groups displayed on the surface of BPDAs directly affects the optical properties of the self-assembling polymers under ambient conditions, giving rise to the unique color and absorption spectrum of each polymer (Figure 3A & 3B). This is presumably due to the different hydrogen-bonding and electrostatic interactions at the polar surfaces of the assembly that either strengthen or weaken the van der Waals association between lipid monomers. The balance between these intermolecular forces results in various degrees of crystallinity in lipid packing arrangements, and therefore, different effective conjugation lengths upon UV-polymerization.

BPDA-1, modified with *L*-aspartate residues, showed very different optical properties than a previously reported BPDA system modified with *L*-glutamate residues.[24] The glutamate modified BPDA absorbed strongly at 630 nm and displayed an intense blue color. With two carboxylate groups more closely spaced at the polar end, the aspartate-modified **BPDA-1** presumably displayed less favorable hydrogen-bonding and/or stronger electrostatic repulsion between polar surface residues than its glutamate-modified counterpart, significantly reducing the crystallinity of its lipid packing. Disordered packing induced by the unfavorable surface interactions in **BPDA-1** are reflected by its weaker absorption at 630 nm and more intense absorption at 550 nm, or the reduced effective conjugation length of the poly(ene-yne) backbone. In contrast, the strong absorption of **BPDA-3** in its "blue phase" indicates that serine-terminated bolaamphiphiles are packed in an ordered manner with their diacetylene units well-aligned, which upon UV-irradiation, leads to the formation of a polymer with an extended ene-yne conjugation backbone. This may reflect strong hydrogen-bonding interactions at the surface.

In general, polymer ribbons (as opposed to vesicles) are more likely to undergo dramatic conformational reorganization, such as folding, when the polymer backbone continues to propagate upon extended UV irradiation. Unlike vesicular PDAs (e.g., poly-10,12-pentacosadiynoic acid) which do not show a colorimetric response upon UV irradiation with doses less than 0.8 J/cm^2,[13] BPDA

ribbons exhibited optical response to radiation at doses as low as 0.1 J/cm^2. As shown in Fig. 3C, **BPDA-4** demonstrated the most sensitive radiation-induced CR while **BPDA-3** was least sensitive to extended radiation. Again, favorable hydrogen-bonding interactions between neighboring surface serine residues of **BPDA-3** may have contributed to its overall conformational stability, making it the least susceptible to drastic backbone reorganization. In contrast, the neutral hydroxyethyl surface functionality of **BPDA-4** may have conferred additional conformational freedom such that the polymer could fold as the chain propagated.

We have also demonstrated that surface functional groups of BPDAs dramatically influence the colorimetric response of these polymers to pH and thermal perturbations. The sensitive CR of **BPDA-1** in response to elevated pH can be explained by the multiple carboxylic acid residues designed into the monomer. Upon deprotonation, the significant electrostatic repulsion developed between negatively charged carboxylates at the polar surfaces of the polymer likely caused disordering of the lipid side chains. This may lead to distortion of the poly(ene-yne) backbone, reducing the effective conjugation length of **BPDA-1** and resulting in a stronger absorption at the "red phase" region. In comparison, the other three BPDAs showed milder or relatively delayed CR in response to increased pH. More favorable hydrogen bonding between the surface serine residues (**BPDA-3**), the protonation of terminal amine of lysine residues under neutral and mildly acidic conditions (**BPDA-2**), and the surface modification with a neutral hydroxyethyl group (**BPDA-4**) may be stabilizing features that minimize the base-induced CRs of these BPDAs.

We also observed a minor CR at low pH for **BPDA-2**, where the primary amines exposed at the *L*-lysine modified surfaces are significantly protonated under acidic conditions. Electrostatic repulsion between the protonated sites may underscore the observed optical response. Although subtle, this acid-induced CR suggests that it is possible to design the surface chemistry of the BPDAs to drive responses at both low and high pH.

We further demonstrated that a useful range of thermal responsiveness of BPDAs can be obtained through headgroup tuning. The relatively low CR observed above ambient temperature with

BPDA-2, **BPDA-3** and **BPDA-4** makes them good candidates as colorimetric biosensor scaffolds. They can easily withstand incubation at 37 ºC or higher without presenting significant background CR. The strikingly different thermochromatic behaviors of aspartate-terminated **BPDA-1** and serine-terminated **BPDA-3** underscores the power of hydrogen bonding and Coulombic interactions in controlling the properties of self-assembling polymers. Unfavorable Coulombic interactions at the surface of **BPDA-1** could contribute to the destabilization of the polymer backbone, lowering the transition energy barrier for an optical response to occur. Therefore, even a slight temperature increase (e.g. from rt to 35 ºC) led to a quite significant optical response of **BPDA-1** (20% CR) (Fig. 6). Presumably, the side chain packing arrangement of **BPDA-1** was completely altered upon thermal activation, resulting in a drastically different effective conjugation length of the backbone. In contrast, with favorable hydrogen-bonding interactions at the polar surface of **BPDA-3**, an irreversible color change only occurred at a much higher temperature (e.g. 20% CR at 90 ºC) when the hydrogen-bonding network was presumably disrupted.

It is worth noting that with 0.1 J/cm^2 radiation dose, not all lipids were polymerized to the same extent. Such 'incomplete' polymerization could also have a direct impact on the stability of the polymer backbone, and therefore affect both the onset and the extent of CR of BPDAs to environmental perturbations.

Finally, our work also provides insights into the mechanism of chromatic tranisitions of PDAs, which remains controversial despite numerous studies in the literature. A widely accepted model attributes shortening of effective conjugation length to an increase in lattice strain,[27] often induced by conformational disorder of the side chains on a conjugated PDA backbone.[28-30] However, recent infrared spectroscopy and AFM studies of PDA films suggest that the side chains of "red phase" PDAs induced by thermal treatment are in an equally or more ordered conformation than those in "blue phase" PDAs.[7,8] A compromised explanation suggests that the alkyl side chains in the "red phase" remain in an ordered conformation, with only a slightly different packing mode from the "blue

phase".[31] More recent investigation of the temperature dependence of visible absorption spectra and the electron diffractions of PDA films revealed that the electronic natures of the PDAs are strongly dependent on their resonance backbone structures as well as the stacking of the main chains.[8] Leblanc *et al.* proposed that extended radiation-induced chromatic changes of PDAs may arise from "self-folding" of the originally linear conjugation backbone into a zigzag structure (via the free rotation of single bonds) upon propagation of the polymer chain, resulting in a shortened π-electron delocalization.[31]

In this study, the dramatic morphological transformation of BPDAs from ribbons to nanofibers accompanying the charge-induced CR (Fig. 5) suggest that both side chain disordering and disruption of main chain packing play important roles in the observed chromatic shift. This phenomenon was previously observed in a BPDA system functionalized with *L*-glutamate residues at the polar surfaces.[24] It was proposed that the polymer fibers formed upon base treatment, roughly 10 nm in width, adopt a tubular micellar conformation with conjugated polymer backbones as a rigid core and saturated lipid side chains as floppy arms capped with charged headgroups.[24] Interestingly, we did not observe any morphological transformation accompanying thermally-induced CR of any BPDAs studied here. This suggests that disruption of effective conjugation via temperature increase may proceed by a different mechanism, perhaps by a change in side chain packing modes. Such side chain reorganization does not necessarily lead to the disordering of side chains. Instead, side chain packing could become more crystalline upon heat treatment as suggested by others.[7] Finally, the radiation dose-induced CR observed with BPDAs (Fig. 3C) may have arisen from the zigzagging or self-folding of the growing backbone as the polymerization proceeds.

In conclusion, we have shown that by designing appropriate functional groups at the surface of BPDA assemblies, it is possible to fine tune the robustness or optical responsiveness of the self-assembling conjugated polymer towards environmental perturbations. These results provide a basis to either enhance or suppress acute optical responses or morphological transformations of BPDAs in response to environmental stimuli, meeting the requirements of various sensing applications. This

work establishes a foundation for construction of colorimetric biosensors that detect biological pathogens with high sensitivity and signal-to-noise ratio.

Experimental section:

Materials. 10,12-Docosadiynedioic acid was obtained in 95% purity from Lancaster and converted to N-hydroxysuccinimide activated lipid **5** following a literature protocol.[24] Water used in the preparation of various self-assembled polymers was purified with a Millipore Milli-Q system.

Synthesis.

General Techniques. Analytical thin-layer chromatography (TLC) was conducted on Sigma-Aldrich silica gel aluminum plates (60 Å, with fluorescent indicator) with detection by UV light and phosphomolybdic acid (PMA, 10% in EtOH). For flash chromatography, 60 Å silica gel (Merck, 230-400 mesh) was employed. Reversed-phase high-pressure liquid chromatography (RP-HPLC) was performed on a Rainin Dynamax SD-200 HPLC system using Microsorb and Dynamax C_{18} reversed phase columns and UV detection was performed with a Rainin Dynamax UV-1 detector. Yields refer to chromatographically and spectroscopically (^{1}H NMR) homogeneous materials. NMR spectra were recorded on a Bruker DRX-500 spectrometer. Chemical shifts are reported relative to the major solvent peak when a mixed NMR solvent system was employed. Low-resolution electrospray ionization mass spectrometry (ESI-MS) was performed on a Hewlett-Packard 1100 mass spectrometer. High-resolution mass spectra (HRMS) were recorded at the Mass Spectrometry Facility at the University of California at Berkeley using either fast atom bombardment (FAB) or electrospray ionization (ESI).

Compound 6. Triethylamine (~ 0.1 mL) was added to a solution of *L*-Asp(OEt)$_2$ (99.6 mg, 0.441 mmol) in 15 mL of THF and 0.2 mL H_2O. The Asp(OEt)$_2$ solution was then added dropwise to lipid **5** (212 mg, 0.462 mmol) in THF (67 mL). The reaction was stirred at rt for 18 h before 1 N HCl was added to adjust the pH to 5. The product was concentrated using rotary evaporation and purified using flash chromatography (39:1 $CHCl_3$:MeOH, R_f 0.3) in 36% yield (84.0 mg, 0.157 mmol). ^{1}H

NMR (500 MHz, $CDCl_3$): δ 6.53 (1H, d, *J* = 5.0 Hz), 4.84 (1H, m), 4.21 (2H, m), 4.14 (2H, dd, *J* = 15.0, 10.0 Hz), 3.01 (1H, dd, *J* = 15.0, 5.0 Hz), 2.83 (1H, dd, *J* = 20.0, 5.0 Hz), 2.33 (2H, t, *J* = 7.5 Hz), 2.23 (6H, m), 1.61 (4H, m), 1.49 (4H, m), 1.36 (22H, m); ^{13}C NMR (125 MHz, $CDCl_3$): δ 178.80, 173.06, 171.16, 170.83, 77.44, 77.20, 65.28, 65.24, 61.84, 61.00, 48.42, 36.43, 36.34, 29.11, 29.05, 28.93, 28.88, 28.79, 28.71, 28.65, 28.25, 28.20, 25.48, 24.64, 19.14, 14.09, 14.03; LRMS ESI$^+$: $C_{30}H_{48}NO_7$ $[M+H]^+$, calcd 534, found 534.

Compound 1. Compound **6** (84.0 mg, 0.157 mmol) was dissolved in 2:1/THF:H_2O (30 mL) and adjusted to pH 11 with 2 N KOH. The solution was stirred at 45 °C for 4 h before it was quenched by Amberjet IR-120 (H^+ form) ion-exchange resin to pH 5. The clear solution was collected and concentrated by rotary evaporation which yielded 74.0 mg (0.155 mmol, 99%) of the final product. ^{1}H NMR (500 MHz, 5:3/CD_3OD:$CDCl_3$ with trace D_2O): δ 4.72 (1H, m), 2.88 (1H, dd, *J* = 17.0, 6.0 Hz), 2.82 (1H, dd, *J* = 17.0, 5.0 Hz), 2.27 (2H, t, *J* = 7.5 Hz), 2.22 (6H, m), 1.59 (4H, m), 1.520 (4H, m), 1.36 (4H, m), 1.3 (12H, m); ^{13}C NMR (125 MHz, 5:3/CD_3OD:$CDCl_3$ with trace D_2O): δ 177.78, 175.69, 174.17, 174.01, 78.04, 78.00, 66.08, 66.05, 36.74, 36.67, 35.01, 34.83, 30.83, 29.91, 29.88, 29.84, 29.65, 29.61, 29.48, 29.43, 29.05, 29.02, 26.36, 25.64, 19.67; HRMS ESI$^-$: $[M-H]^-$ $C_{26}H_{38}NO_7$ calcd 476.2654, found 476.2637.

Compound 7. Lipid **5** (321 mg, 0.699 mmol) was dissolved in 3:1/THF:H_2O (50 mL), to which *N*-ε-trifluoroacetyl-*L*-lysine (203 mg, 0.840 mmol) was subsequently added. Addition of 1 M KOH solubilized all reactants in the mixed solvent system at pH 9. The reaction was allowed to proceed at rt and product formation was monitored by TLC (7:2/$CHCl_3$: MeOH, R_f 0.42). After 24 h, the product was concentrated in vacuo and purified by flash chromatography (10:1/CH_2Cl_2:MeOH followed by 5:1/CH_2Cl_2:MeOH, R_f 0.2) in 62% yield (254 mg). ^{1}H NMR (500 MHz, CD_3OD): δ 4.36 (1H, m), 3.27 (2H, t, *J* = 7.0 Hz), 2.27 (2H, t, *J* = 7.5 Hz), 2.23 (6H, m), 1.86 (1H, m), 1.69 (2H, m), 1.59 (5H, m), 1.49 (4H, m), 1.38 (6H, m), 1.32 (12H, m); ^{13}C NMR (125 MHz, CD_3OD): δ 177.64, 176.34, 175.45,

158.93 (q, J = 36.25 Hz), 117.44 (q, J = 285 Hz) , 77.78, 77.76, 66.37, 66.34, 49.85, 40.39, 36.72, 34.98, 32.06, 30.19, 30.18, 30.11, 30.09, 29.96, 29.92, 29.76, 29.74, 29.43, 29.41, 29.27, 26.83, 25.98, 24.06, 19.66; LRMS ESI$^+$: $C_{30}H_{46}N_2O_6F_3$ $[M+H]^+$, calcd 588, found 588.

Compound 2. Compound **7** (254 mg, 0.433 mmol) was dissolved in 10:5:1/H_2O:THF:MeOH (64 mL) and the pH of the solution was adjusted to 12-13 with 1 M KOH. The reaction mixture was stirred at 35 ^oC and product formation was monitored by TLC (3:2/$CHCl_3$:MeOH, R_f 0.13). The reaction was quenched after 12 h via the addition of Amberjet IR-120 (H^+ form) ion-exchange resin to pH 4. Crude product was concentrated and purified by reversed-phase (C_{18}) HPLC. Lipid **2** (98 mg) was isolated in 46% yield. ^{1}H NMR (500 MHz, 3:2/CD_3OD:$CDCl_3$): δ 4.25 (1H, m), 2.86 (2H, t, J = 7.5 Hz), 2.25 (2H, t, J = 7.5 Hz), 2.21 (6H, m), 1.80 (1H, m), 1.67 (2H, m), 1.58 (5H, m), 1.48 (4H, m), 1.37 (6H, m), 1.30 (12H, m); ^{13}C NMR (125 MHz, 3:2/CD_3OD:$CDCl_3$): δ 175.49, 175.46, 174.84, 77.68, 77.65, 66.09, 66.08, 40.07, 37.20, 32.77, 30.39, 30.40, 30.39, 29.93, 29.91, 29.87, 29.83, 29.67, 29.61, 29.46, 29.42, 29.07, 29.04, 27.40, 26.56, 25.83, 22.65, 19.56; HRMS ESI$^+$: $C_{28}H_{47}N_2O_5$ $[M+H]^+$, calcd 491.3479, found 491.3486.

Compound 3. Lipid **5** (606 mg, 1.32 mmol) was dissolved in THF (50 mL), to which an aqueous solution of *L*-serine (140 mg, 1.33 mmol) at pH 9-10 (via the addition of triethylamine) was subsequently added. The reaction was allowed to stir at rt for 4 h and product formation was monitored by TLC (2:1/CH_2Cl_2: MeOH, R_f 0.5). The crude product was neutralized with Amberlite IR-120 (H^+ form) ion exchange resin and then concentrated in vacuo. Flash column chromatography sequentially eluting with 9:1/CH_2Cl_2:MeOH, 4:1/CH_2Cl_2:MeOH and 2:1 /CH_2Cl_2:MeOH) afforded isolated product (412 mg) in 69% yield. ^{1}H NMR (500 MHz, 3:1/CD_3OD:$CDCl_3$): δ 4.29 (1H, t, J = 5.0 Hz), 3.85 (1H, dd, J = 10.5, 5.0 Hz), 3.76 (1H, dd, J = 10.5, 5.5 Hz), 2.24 (8H, m), 1.61 (4H, m), 1.51 (4H, m), 1.37 (4H, m), 1.29 (12H, m); ^{13}C NMR (125 MHz, 3:1/CD_3OD:$CDCl_3$): δ 178.95, 175.92, 174.36, 77.52, 77.49, 65.35, 63.71, 58.74, 56.19, 45.55, 36.57, 35.76, 29.37, 29.31, 29.26, 29.01, 28.84, 28.82, 28.38,

28.36, 25.71, 25.60, 19.18; HRMS ESI$^+$: $C_{25}H_{40}NO_6$ $[M+H]^+$, calcd 450.2856, found 450.2861.

Compound 4. One equivalent of ethanolamine (48 μL) was added to 10 mL of a solution of lipid **5** (323 mg, 0.704 mmol) in THF. Upon the addition, white precipitates immediately formed. Triethyamine and water were added dropwise to raise the pH to 8-9 and solubilize the reaction mixture. The reaction was allowed to stir at rt for 2 h before neutralized with Amberlite IR-120 (H^+ form) ion exchange resin and concentrated in vacuo. Flash column chromatography sequentially eluting with 9:1/$CHCl_3$:MeOH and 4:1/$CHCl_3$:MeOH afforded the product (280 mg) in 98% yield. ^{1}H NMR (500 MHz, $CDCl_3$ with trace CD_3OD): δ 3.62 (2H, t, *J* = 5.5 Hz), 3.32 (2H, t, *J* = 5.5 Hz), 2.25 (2H, t, *J* = 7.5 Hz), 2.19 (4H, t, *J* = 7.0 Hz), 2.15 (2H, t, *J* = 7.5 Hz), 1.56 (4H, m), 1.45 (4H, m), 1.32 (4H, m), 1.25 (12H, m); ^{13}C NMR (125 MHz, $CDCl_3$ with trace CD_3OD): δ 176.62, 174.74, 77.41, 77.19, 65.21, 61.60, 41.87, 36.44, 33.88, 29.08, 29.06, 28.96, 28.90, 28.83, 28.73, 28.61, 28.55, 28.15, 28.10, 25.60, 24.75, 19.05; HRMS FAB$^+$ (NBA): $C_{24}O_4NH_{40}$ $[M+H]^+$, calcd 406.2957, found 406.2963.

Self-assembly of lipids and polymerization. Aqueous NaCl (0.1 N, 2 mL) was added to 0.6 mg of each bolaamphiphile. The mixture was sonicated for 10 min with a 40W probe sonicator. The resulting clear solution was allowed to cool to rt and incubated at 4 °C for 40 min.

Freshly prepared supramolecular aggregates were irradiated with UV light (254 nm, CL 1000 Ultraviolet Crosslinker). Polymerization occurred rapidly for all BPDAs and colors from blue to purple developed with a 0.05 J/cm^2 radiation dose. Higher radiation doses (0.1, 0.2, 0.4, 0.6, 0.8, 1.0, 1.5 and 2.0 J/cm^2) were also applied to investigate radiation dose-induced chromatic shifts of BPDAs. Averaged results from six replicates were used to generate radiation dose-CR curves.

UV-Visible Spectroscopy. Visible absorption spectra were recorded on a Shimadzu UV-1601 spectrometer under ambient conditions. BPDAs (0.3 mg/mL, 0.1 N aq. NaCl) were diluted 10-fold (with 0.1 N aq. NaCl) before the absorption spectrum was recorded.

pH- and thermally-induced colorimetric responses (CR). Freshly polymerized BPDA

solutions (0.3 mg/mL in 0.1 N NaCl, 0.1 J/cm^2 radiation dose) were loaded on a 96-well polystyrene microtiter plate (50 μL per well). An equal volume of potassium hydroxide solution (with a gradient of [OH^-] from 1 M to 10^{-4} M) or hydrochloric acid solution (with a gradient of [H^+] from 1 M to 10^{-4} M) was added to each well and mixed with the polymer. The resulting solutions were then subject to CR and pH measurements. Averaged results from two replicates were used for generating the pH-CR curves.

A thermocycler was used to heat BPDA solutions (0.3 mg/mL in 0.1 N NaCl) loaded onto a polycarbonate microtiter plate (100 μL/well) to target temperatures (ranging from 30 to 90 °C) at a fixed heating rate (1 °C/sec) and then maintained at the target temperature for 1 min. The BPDA solutions were then transferred to a 96-well polystyrene microtiter plate and subject to CR measurements. Averaged results from three replicates were used to generate temperature-CR curves.

The CR was recorded on a SPECTRAmax™ 250 Microplate Spectrophotometer supported by SOFTmax PRO Microplate Analysis software (Molecular Devices Corporation). CR was measured as the percent change in the absorption at 630 nm ("blue phase" BPDA) relative to the total absorption at 630 nm and 550 nm ("red phase" BPDA). The initial percentage of "blue phase" at ambient condition before acid/base addition is defined as $B_0 = I_{630} / (I_{630} + I_{550})$. The same value was calculated for the solution subjected to pH or thermal perturbations (B_p). CR is therefore defined as the percentage change in "blue phase" (B) upon perturbations: $CR = [(B_0 - B_p) / B_0] \times 100\%$.

Transmission Electron Microscopy (TEM). TEM images of all BPDAs studied here were obtained on a Philips CM200/FEG microscope (operating at 200 kV) at the National Center for Electron Microscopy. Samples were freshly made and deposited on holey-carbon film-coated Cu grids purchased from TED PELLA, Inc. (Redding, CA). Although the microstructures of diacetylene lipids are visualizable owing to the high electron density, staining with 0.5% uranyl acetate was performed to enhance the image quality.

Acknowledgements:

This work was supported by the Laboratory Directed Research and Development Program of Lawrence Berkeley National Laboratory under the Department of Energy Contract No. DE-AC03-76SF00098. The authors acknowledge support of the staff and facilities at the National Center for Electron Microscopy, Lawrence Berkley National Laboratory.

REFERENCES

(1) (i) Ringsdorf, H.; Schlarb, B.; Venzmer, J. *Angew. Chem. Int. Ed. Engl.* **1988**, *27*, 113-158.
(ii) Fendler, J. H. *Biomimetic Membranes:* Wiley, New York, 1982.
(iii) Special section, "Engineering a Small World", *Science* **1991**, *254*, 1300-1335.
(iv) Song, X.; Nolan, J.; Swanson, B. I. *J. Am. Chem. Soc*. **1998**, *120*, 4813-4814 and 11314-11315.
(v) Miller, A. D. *Angew. Chem., Int. Ed. Engl.* **1998**, *37*, 1768-1785.
(2) Charych, D. H.; Nagy, J. O.; Spevak, W.; Bednarski, M. D. *Science* **1993**, *261*, 585-588.
(3) Berman, A.; Ahn, D. J.; Lio, A.; Salmeron, M.; Reichert, A.; Charych, D. *Science* **1995**, *269*, 515-518.
(4) Itoh, C.; Kondoh, T.; Tanimura, K. *Chem. Phys. Lett.* **1996**, *261*, 191-194.
(5) Lapersonne-Meyer, C. *Int. J. Modern Phys. B* **2001**, *15*, 3593-3596.
(6) Tieke, B.; Graf, H. J.; Wegner, G.; Naegele, B.; Ringsdorf, H.; Banerjie, A.; Day, D.; Lando, J. B. *Colloid Polym. Sci.* **1977**, *255*, 521-531.
(7) Lio, A.; Reichert, A.; Ahn, D. J.; Nagy, J. O.; Salmeron, M.; Charych, D. H. *Langmuir* **1997**, *13*, 6524-6532.
(8) Kuriyama, K.; Kikuchi, H.; Kajiyama, T. *Langmuir* **1998**, *14*, 1130-1138.
(9) Batchelder, D. N.; Evans, S. D.; Freeman, T. L.; Haeussling, L.; Ringsdorf, H.; Wolf, H. *J. Am. Chem. Soc.* **1994**, *116*, 1050-1053.
(10) Singh, A.; Thompson, R. B.; Schnur, J. M. *J. Am. Chem. Soc.* **1986**, *108*, 2785-2787.
(11) Spevak, W.; Nagy, J. O.; Charych, D. H.; Schaefer, M. E.; Gilbert, J. H.; Bednarski, M. D. *J. Am. Chem. Soc.* **1993**, *115*, 1146-1147.
(12) Cheng, Q.; Stevens, R. C. *Langmuir* **1998**, *14*, 1974-1976.
(13) Okada, S.; Peng, S.; Spevak, W.; Charych, D. *Acc. Chem. Res.* **1998**, *31*, 229-239.
(14) Cheng, Q.; Yamamoto, M.; Stevens, R. C. *Langmuir* **2000**, *16*, 5333-5342.
(15) Song, J.; Cheng, Q.; Stevens, R. C. *Chem. Phys. Lipids* **2002**, *114*.
(16) Stanish, I.; Santos, J. P.; Singh, A. *J. Am. Chem. Soc.* **2001**, *123*, 1008-1009.
(17) Kim, J.-M.; Ji, E.-K.; Woo, S. M.; Lee, H.; Ahn, D. J. *Adv. Mater.* **2003**, *15*, 1118-1121.
(18) Wenzel, M.; Atkinson, G. H. *J. Am. Chem. Soc.* **1989**, *111*, 6123-6127.
(19) Carpick, R. W.; Mayer, T. M.; Sasaki, D. Y.; Burns, A. R. *Langmuir* **2000**, *16*, 4639-4647.
(20) Carpick, R. W.; Sasaki, D. Y.; Burns, A. R. *Langmuir* **2000**, *16*, 1270-1278.
(21) Charych, D.; Cheng, Q.; Reichert, A.; Kuziemko, G.; Stroh, M.; Nagy, J. O.; Spevak, W.; Stevens, R. C. *Chem. Biol.* **1996**, *3*, 113-120.
(22) Song, J.; Cheng, Q.; Zhu, S. M.; Stevens, R. C. *Biomed. Microdevices* **2002**, *4*, 213-221.
(23) Mino, N.; Tamura, H.; Ogawa, K. *Langmuir* **1992**, *8*, 594-598.

(24) Song, J.; Cheng, Q.; Kopta, S.; Stevens, R. C. *J. Am. Chem. Soc.* **2001**, *123*, 3205-3213.
(25) Hou, D. R.; Reibenspies, J. H.; Burgess, K. *J. Org. Chem.* **2001**, *66*, 206-215.
(26) Langworthy, T. A. *Curr. Topics in Membr. Transp.* **1982**, *17*, 45-77.
(27) Eckhardt, H.; Boudreaux, D. S.; Chance, R. R. *J. Chem. Phys.* **1986**, *85*, 4116-4119.
(28) Tomioka, Y.; Tanaka, N.; Imazeki, S. *J. Chem. Phys.* **1989**, *91*, 5694-5700.
(29) Tokura, Y.; Nishikawa, S.; Koda, T. *Solid State Commun.* **1986**, *59*, 393-395.
(30) Foley, J. L.; Li, L.; Sandman, D. J.; Vela, M. J.; Foxman, B. M.; Albro, R.; Eckhardt, C. J. *J. Am. Chem. Soc.* **1999**, *121*, 7262-7263.
(31) Huo, Q.; Russell, K. C.; Leblanc, R. M. *Langmuir* **1999**, *15*, 3972-3980.

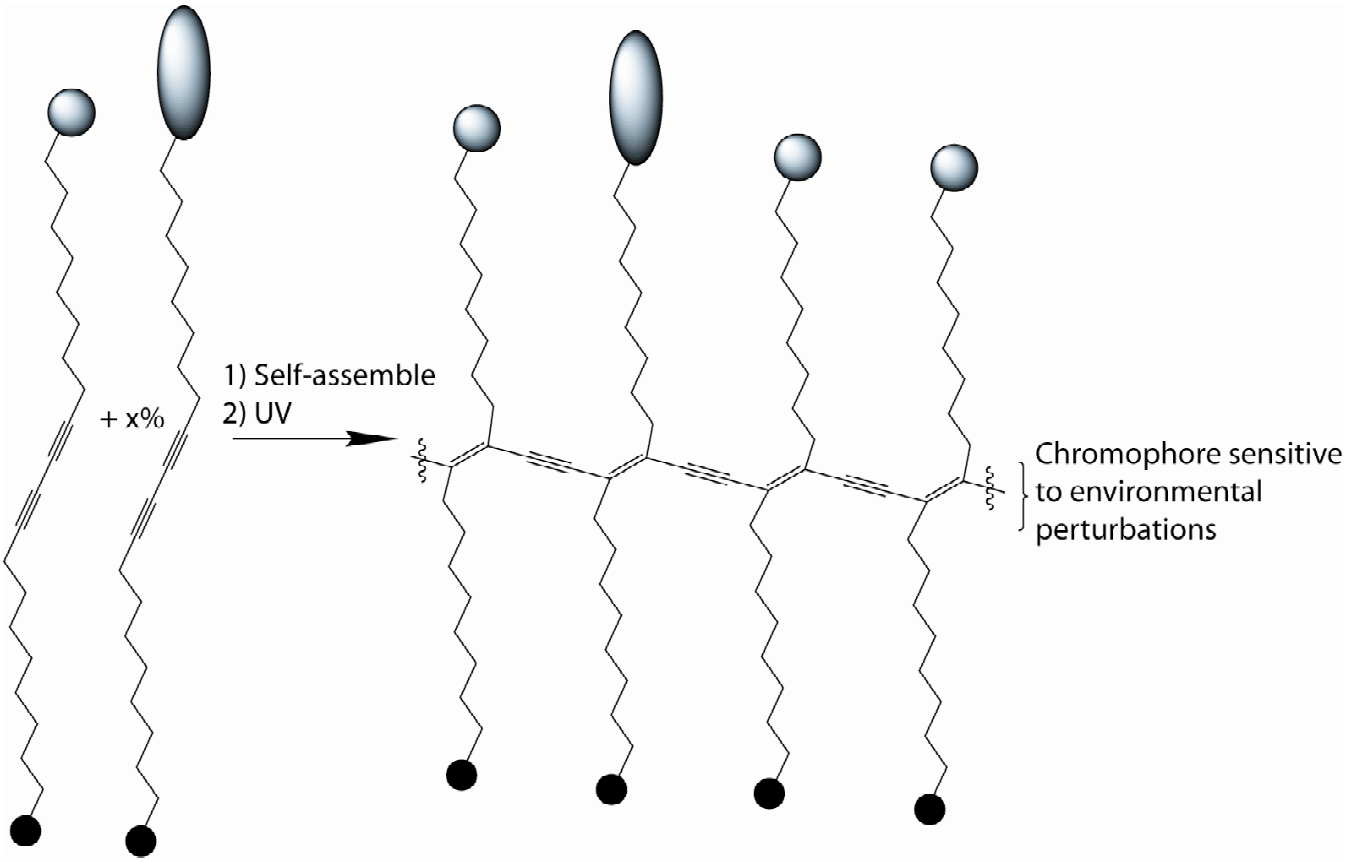


Figure 1. Assembly and polymerization of amphiphilic or bolaamphiphilic diacetylene lipids. Circles and ovals represent functional groups of different size and nature. In the case of amphiphilic lipids, black circles represent the termini of hydrocarbon chains, while in the case of bolaamphiphilic lipids, gray and black circles are both polar residues of identical or different nature. Gray ovals, incorporated at a defined percentage (x%), represent synthetic ligands for receptor binding. The poly(ene-yne) system undergoes colorimetric changes in response to environmental perturbations including temperature, pH and specific ligand-pathogen binding events. This cartoon depiction does not reflect the actual lipid packing arrangement of BPDAs, which could be either parallel, antiparallel, or a combination of the two.

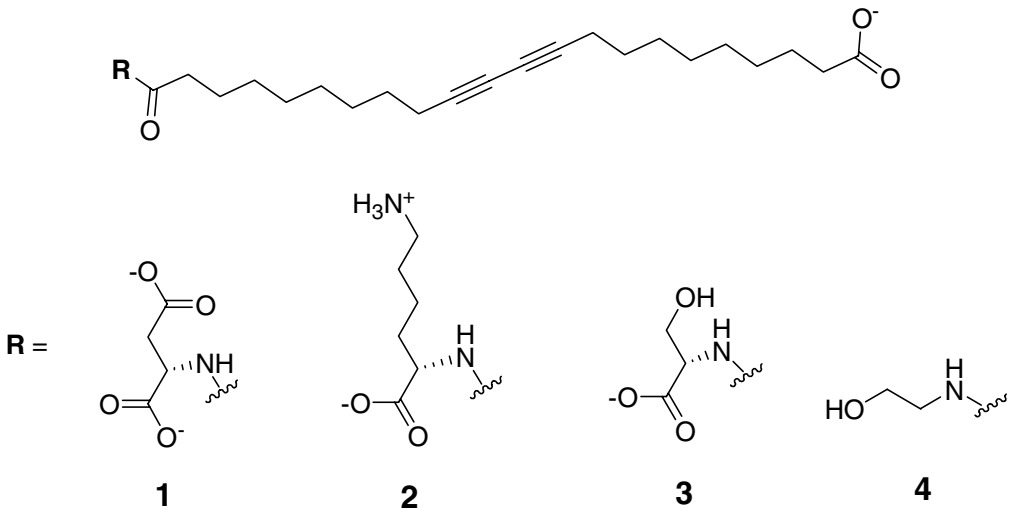
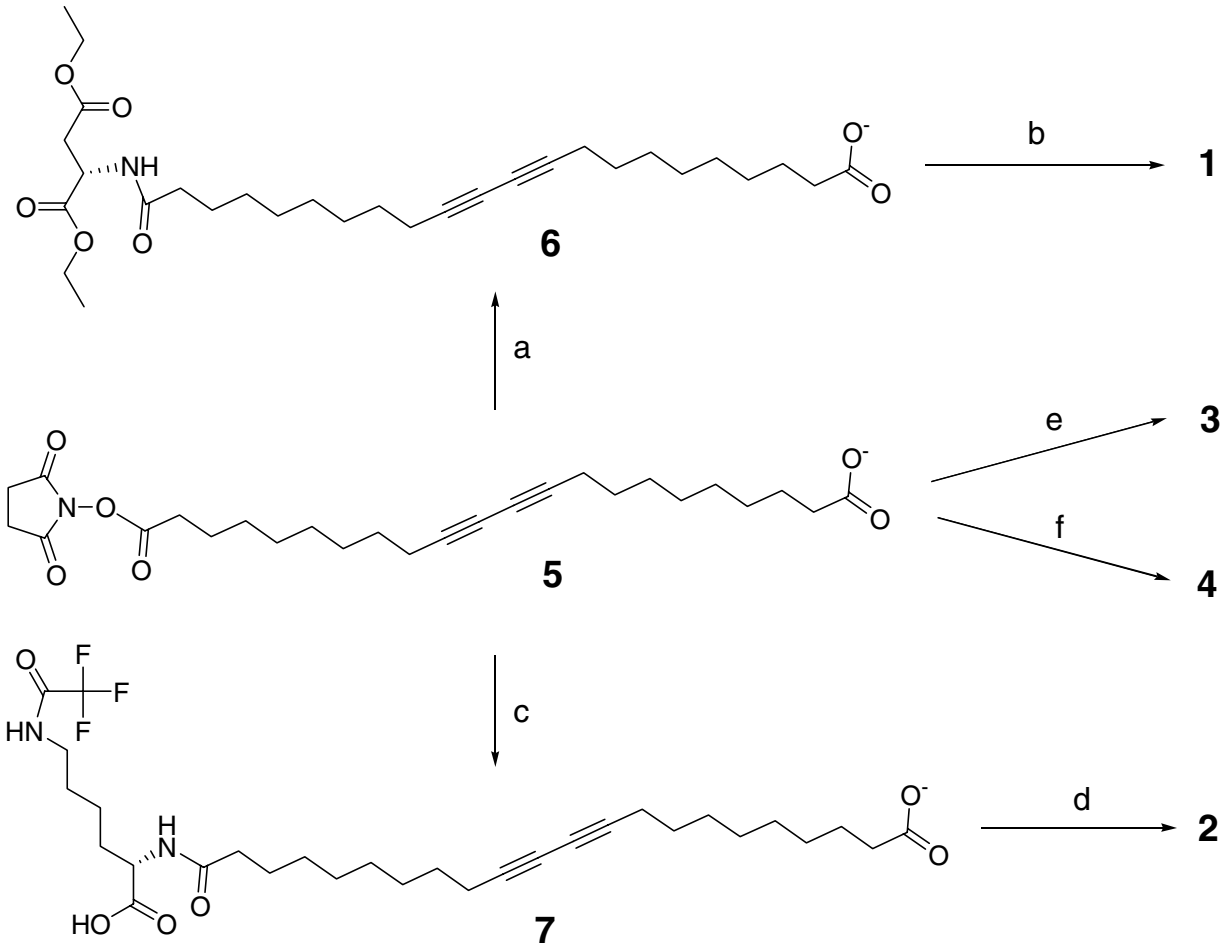
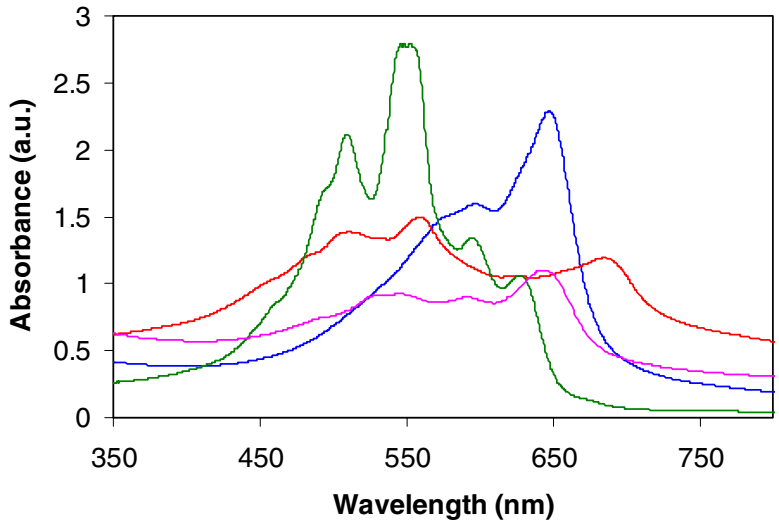


Figure 2. Bolaamphiphilic diacetylene lipids 1-4 with various headgroup modifications.

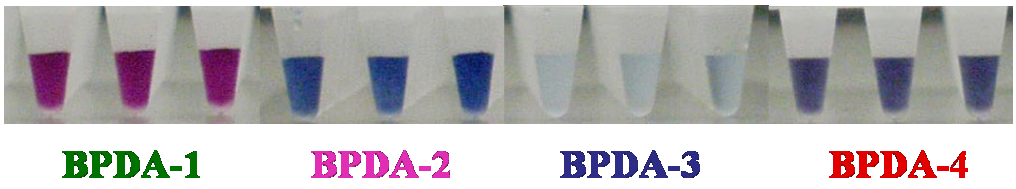


Scheme 1. Synthesis of targets 1-4. *Reagents and conditions*: (a) 0.95 equiv. *L*-Asp$(OEt)_2$, Et_3N, THF with 0.2% H_2O (v/v), rt, 18 h, 36%; (b) THF:H_2O/2:1 (v/v), pH 11 (KOH), 45 ºC, 4 h, 99%; (c) 1.2 equiv. *N*-ε-trifluoroacetyl-*L*-lysine, pH 9 (KOH), THF:H_2O/3:1 (v/v), rt, 24 h, 62%; (d) H_2O:THF:MeOH/10:5:1 (v/v), pH 12-13 (KOH), 35 ºC, 12 h, 46%; (e) 1 equiv. *L*-Serine, Et_3N, THF, rt 4 h, 69%; (f) 1 equiv. ethanolamine, Et_3N, THF, rt 2 h, 98%.

(A)


Absorbance (a.u.)
3
2.5
2
1.5
1
0.5
0
350
450
550
650
750
Wavelength (nm)

(B)


BPDA-1
BPDA-2
BPDA-3
BPDA-4

(C)

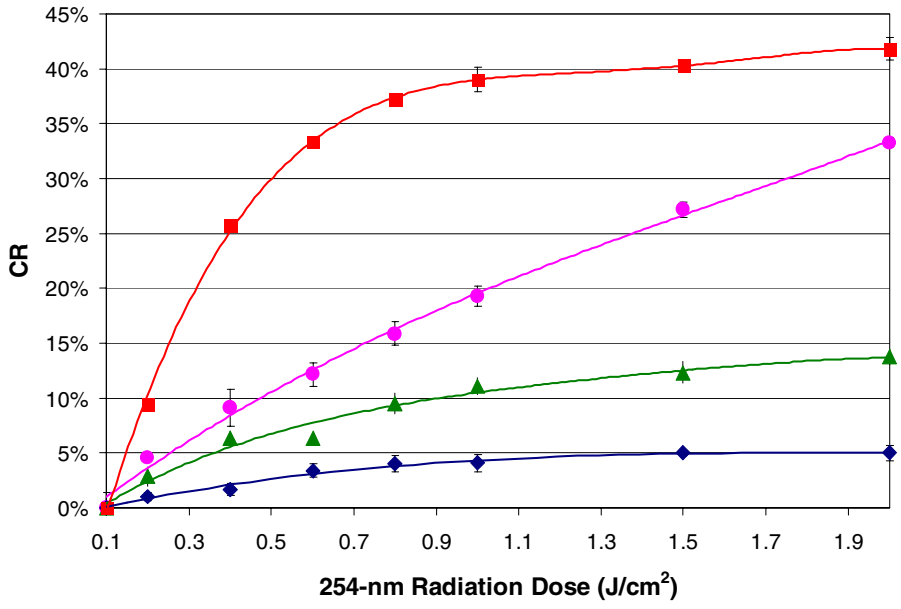

CR
45%
40%
35%
30%
25%
20%
15%
10%
5%
0%
0.1
0.3
0.5
0.7
0.9
1.1
1.3
1.5
1.7
1.9
254-nm Radiation Dose (J/cm2)

Figure 3. (A) Visible spectra of BPDAs formed with 0.1 J/cm^2 UV irradiation. BPDA-1 (Green); BPDA-2 (pink); BPDA-3 (blue); BPDA-4 (red). a.u. = arbitrary units. **(B) BPDAs formed with 0.1 J/cm^2 UV irradiation display various shades of blue (BPDA-2, BPDA-3 and BPDA-4) and purple (BPDA-1) at ambient conditions. (C) Radiation dose-induced colorimetric response of BPDAs. BPDA-1** (green triangle); **BPDA-2** (pink circle); **BPDA-3** (blue diamond); **BPDA-4** (red square). Error bars indicate the standard deviation of six replicate experiments.

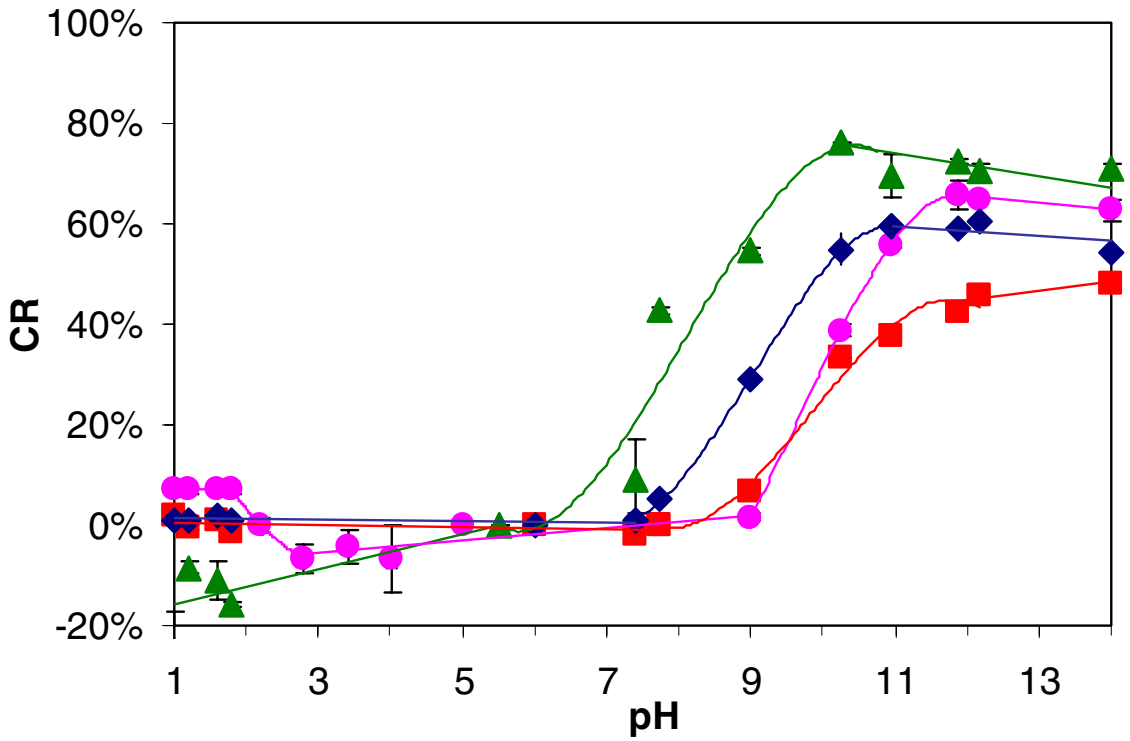


Figure 4. pH-Induced colorimetric response (CR) of various BPDAs. All BPDAs were formed with 0.1 J/cm^2 radiation at 254 nm. **BPDA-1** (green triangle); **BPDA-2** (pink circle); **BPDA-3** (blue diamond); **BPDA-4** (red square). Bars indicate the high and low values of two replicates.

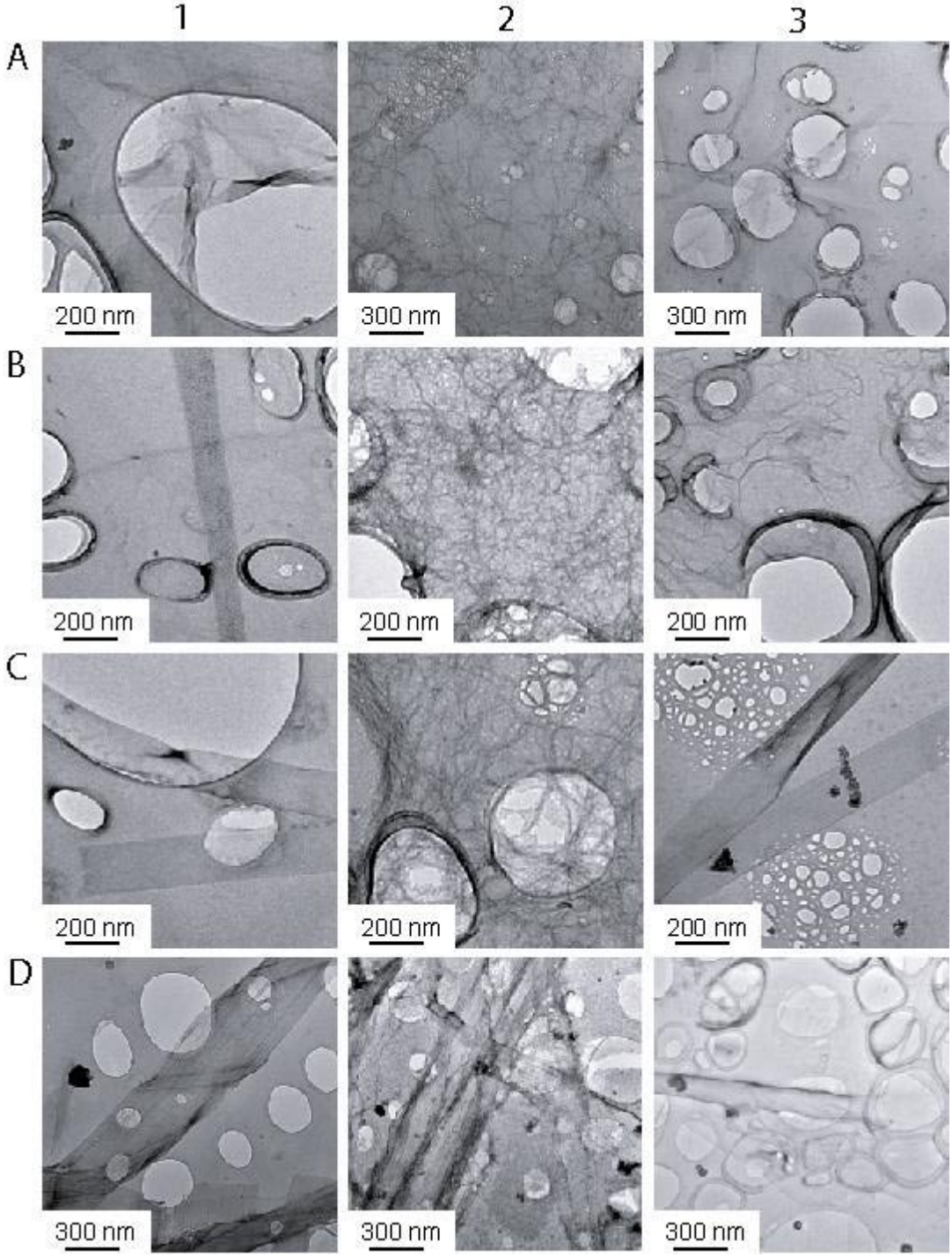
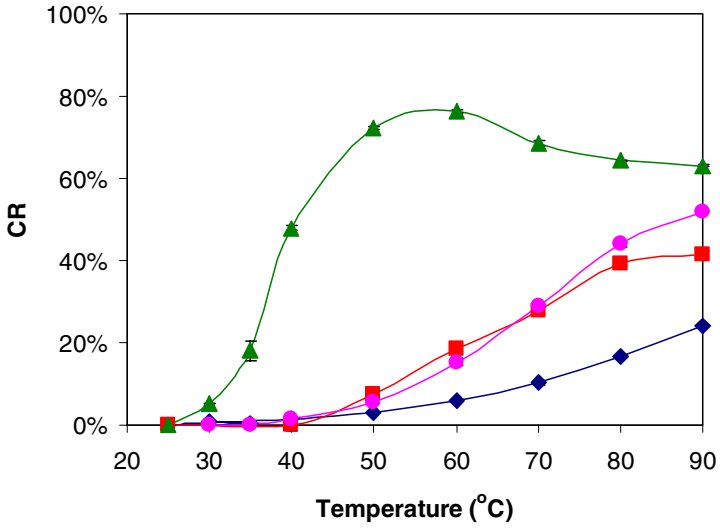


Figure 5. TEM micrographs of BPDAs before and after acid/base treatment. Row A: **BPDA-1;** row B: **BPDA-2;** row C: **BPDA-3;** row D: **BPDA-4.** Column 1: without acid/base treatment; column 2: upon the addition of equal volume of KOH (1 M); column 3: upon the addition of equal volume of HCl (1 M). All BPDAs were formed with 0.1 J/cm^2 radiation at 254 nm. All samples were stained with uranyl acetate.

A



B

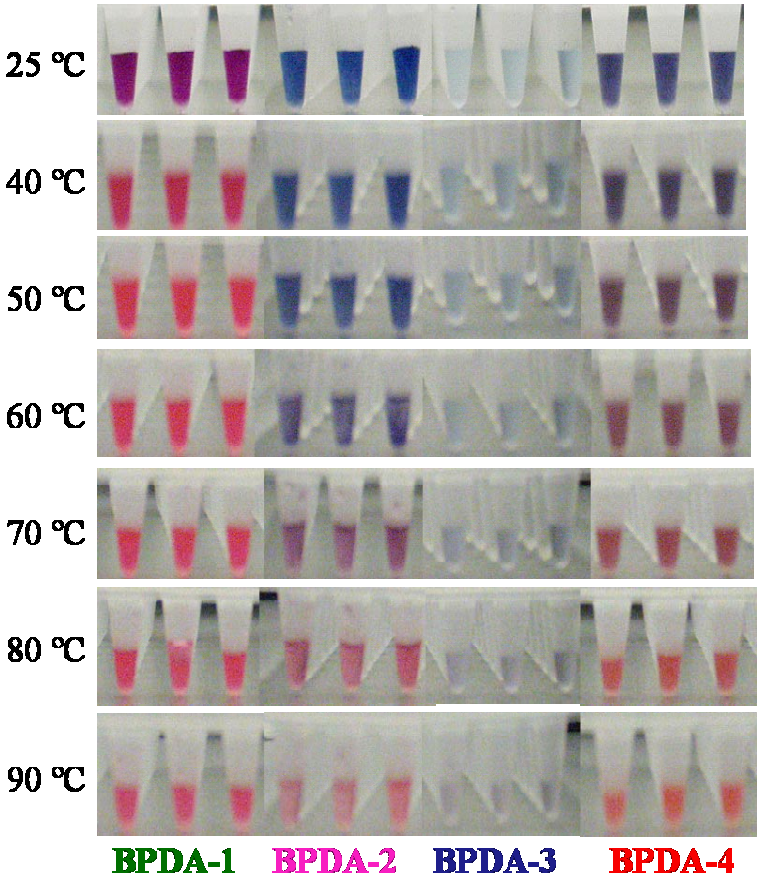
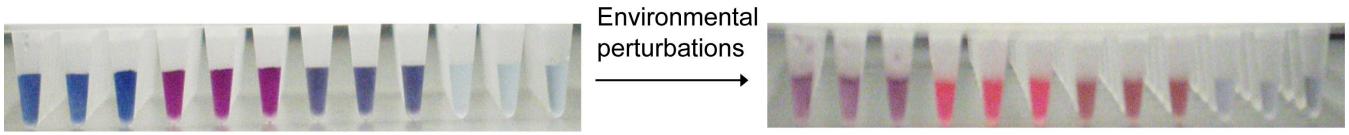


Figure 6. (A) Thermally-induced colorimetric response (CR) of BPDAs. BPDA-1 (green triangle);

BPDA-2 (pink circle); **BPDA-3** (blue diamond); **BPDA-4** (red square). All BPDAs were formed with 0.1 J/cm^2 radiation at 254 nm. Error bars indicate the standard deviation of three replicate experiments. **(B) BPDAs displaying different colors at various temperatures.** All BPDAs were formed with 0.1 J/cm^2 radiation at 254 nm.

TOC graphics:



Functional bolaamphiphilic polydiacetylenes